Hole transporting behavior of Tin (IV) hybrid defect perovskites combining $(CH_3)_3S^+$ cation and halide anions

Mohamed M. Elsenety[1,2], George Belesiotis[1,3], Andreas Kaltzoglou[1], Maria Antoniadou[1], Athanassios G. Kontos[1], Polycarpos Falaras[1,*]

[1]Institute of Nanoscience and Nanotechnology, National Centre for Scientific Research "Demokritos", 15341, Agia Paraskevi Attikis, Athens, Greece

[2]Department of Chemistry, National and Kapodistrian University of Athens, Panepistimiopolis 15771, Zografou, Greece.

[3]School of Chemical Engineering, NTUA, 15780 Zografou, Athens, Greece

(*e-mail: p.falaras@inn.demokritos.gr)

Abstract

Tin(IV)-based, air stable, hybrid, defect perovskites combining trimethyl sulfonium [$(CH_3)_3S^+$] cation with various halide anions (Cl, Br, I) have been synthesized and characterized. The XRPD patterns and corresponding Rietveld analysis show that $((CH_3)_3S)_2SnX_6$ (X = Cl, Br, I, I_5Cl, I_4Cl_2, I_5Br, I_4Br_2) form a cubic 0D framework. According to Raman investigation, their lattice vibrations depend largely on the nature of halogen anion. UV-vis diffuse reflectance spectra confirm that a similar dependence was observed for their band gaps ranging from 1.38 to 4.0 eV. After their physicochemical characterization, the novel perovskites were successfully incorporated as hole-transporting materials in dye-sensitized solar cells (DSCs) using different sensitizers (both organic dyes and transition metal complexes) chemically adsorbed on titania mesoporous electrodes, where power conversion efficiencies as high as 5% were achieved. The obtained results are a significant step towards the development of solution processed, lead-free, solid-state, third generation photovoltaics (dye-sensitized and/or perovskite solar cells), presenting enhanced performance, low fabrication cost and high stability, in contrast to the humidity sensitive methylammonium (MA) and formamidinium (FA) cations, which are commonly used in perovskite solar cells.

Introduction

Perovskite are currently of the most promising materials in 3rd generation photovoltaic technologies and light emitting diodes for highly efficient, simple process and low-cost production[1–3]. Recently, an unprecedented progression of material compositions, engineering modification, and preparation procedures delivered lab-scale solar cell devices that have now reached record power conversion efficiencies up to 24.2% [1,4–9]. However, this type of materials suffers from long-term instability in ambient air due to the hygroscopic amine cations (Methyl ammonium or formamidinium) and from the toxicity of lead [10]. On the other hand, Sn^{4+} atoms in the Cs_2SnI_6 perovskite are more stable and it has been reported either as absorber in perovskite solar cells or as HTM in DSCs with promising power conversion efficiency (PCE) up to 8% [11, 12]. Herein, we report the free-lead perovskite was incorporated in electrolyte-free dye-sensitized solar cells based on the Z907 chromophore chemisorbed onto mesoporous titania electrodes. A power conversion efficiency up to 5% was achieved confirming efficient hole extraction across in DSCs with different type of dye sensitizers, metal-organic (Z907, N719) and organic (MK2, D35).

Experimental Section

Firstly, $(CH_3)_3SCl$, $(CH_3)_3SI$ and SnI_4 were synthesized according to our previous work [13,14]. Secondly, $((CH_3)_3S)_2SnI_{6-x}Cl_x$ and $((CH_3)_3S)_2SnI_{6-x}Br_x$ (x = 1, 2) were prepared by the solid-state synthesis method. All equimolar amounts precursors were ground together and loaded in a silica tube, which was flame-sealed under vacuum and then heated in a furnace at 110 °C for 48 hours.

For solar cell fabrication: All photoanode FTO/TiO_2 cells were prepared as described in our published article [13]. Moreover, 0.1 mol L^{-1} perovskite solutions in DMF were prepared under stirring at 50 °C for 10 minutes. The perovskite solutions were filtered by PTFE 0.45 μm filter. Then, 10.4 μL of TBP and 15 μL of Li-TFSI were added as dopants to increase the conductivity of the $((CH_3)_3S)_2SnI_{6-x}Cl_x$ and $((CH_3)_3S)_2SnI_{6-x}Br_x$ HTMs inside the dye sensitized solar cells.

A drop of the perovskite solution was placed on top of a platinized (100 nm thick prepared by sputtering) FTO glass (cathode electrode) and left to dry at 50 °C. The same procedure was followed for the TiO_2 /dye photoelectrode. The cathode electrode was placed on top of the photoelectrode after an extra drop of the perovskite solution was casted on it.

All first principles calculations, electronic band structure, density of states (DOS), partial density of states (PDOS) were performed using CASTEP code [15].

Results and Discussion

$((CH_3)_3S)_2SnI_{6-x}Cl_x$ and $((CH_3)_3S)_2SnI_{6-x}Br_x$ (x = 0, 1, 2) perovskites were obtained from solid-state synthesis in high crystallinity materials with cubic symmetry (space group $Pa\bar{3}$, (No. 205). No extra peaks of unreacted precursors or other impurities were observed by XRPD analysis in all samples (Figure 1). A small gradual shift of the characteristic peaks around 11.3, 13.1, 26.4 and 27.2° is observed towards higher 2θ values with increasing Cl or Br content.

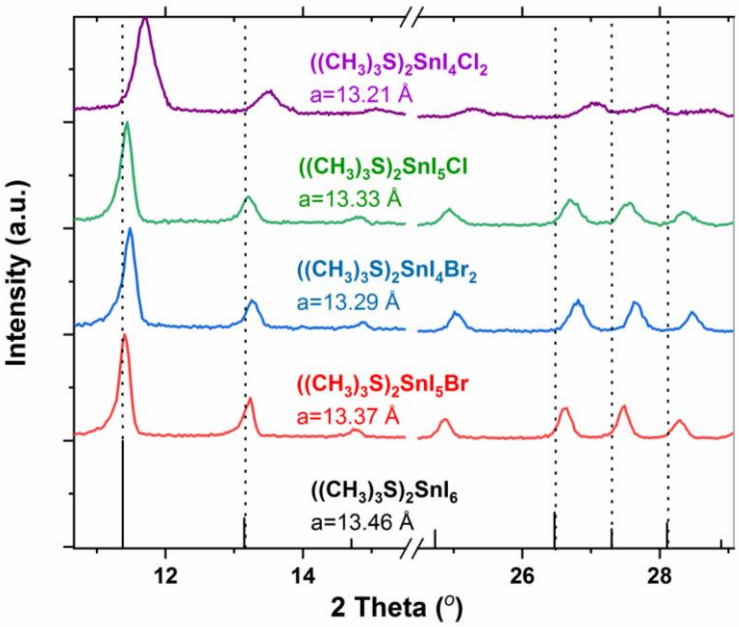

Figure 1. XRPD patterns of trimethyl sulfonium tin perovskites with variable halogen content.

The partial substitution of iodine (ionic radius, I^- = 220 pm) by the smaller chlorine (ionic radius, Cl^- = 181 pm) or bromide (ionic radius, Br^- = 196 pm)[16], leads to the distortion and shrinkage of metal halide octahedra, and consequently, shift of XRD peaks to higher angles. Structural analysis was performed for $((CH_3)_3S)_2SnI_{6-x}Cl_x$ and $((CH_3)_3S)_2SnI_{6-x}Br_x$ (X=0, 1, 2) with the Rietveld method using

initially the structural model of $((CH_3)_3S)_2SnI_6$ without further refinement of the trimethyl sulfonium group.

Micro-Raman spectra (not shown here) of $((CH_3)_3S)_2SnI_{6-x}Cl_x$ and $((CH_3)_3S)_2SnI_{6-x}Br_x$ (X=0, 1, 2) perovskite materials confirm that, two different types of Raman active modes are observed, external vibrations in the $[SnI_{6-x}Cl_x$ or $I_{6-x}Br_x]$ octahedra, which appear at low frequencies (30 – 200 cm^{-1}) as well as internal vibrations in the organic trimethyl sulfonium $(CH_3)_3S$) molecule, at frequencies above 200 cm^{-1}. Moreover, Raman spectra temperature dependence of $((CH_3)_3S)_2SnI_6$ was performed to study lattice vibrational mode and possible phase transition on wide range (-190 to 100 ^oC) of temperature, which predict a phase transition at lower symmetry occurs below -50^oC. The electronic properties of $((CH_3)_3S)_2SnI_{6-x}Cl_x$ and $((CH_3)_3S)_2SnI_{6-x}Br_x$ (X=0, 1, 2) were investigated using UV-Vis spectroscopy at room temperature. Absorption spectra are calculated by transforming the diffuse reflectance spectra to Kubelka-Munk units and presented in Figure 2. By extrapolating the absorption curves to the energy axis, we estimate the bandgap energies which depend largely on the nature of pure halogen anion and slightly increase from 1.43 to 1.50 eV upon partial Iodide substitution.

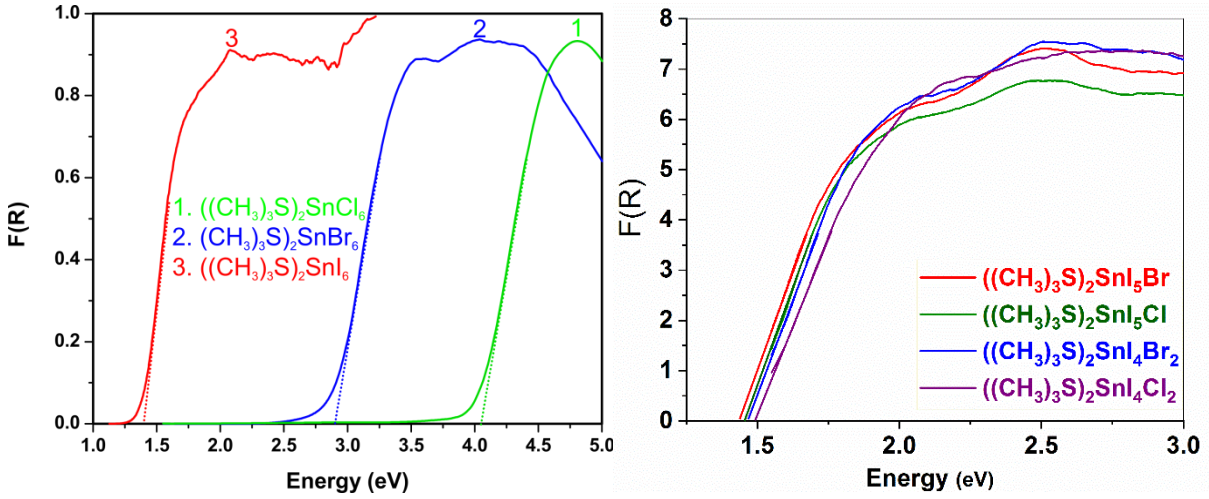

Figure 2. Diffuse reflectance UV-Vis spectra in Kubelka-Munk units for $((CH_3)_3S)_2SnX_6$ (X = Cl, Br, I, I_5Cl, I_4Cl_2, I_5Br, I_4Br_2) perovskite compounds.

The calculated band structure along high G symmetry directions in the first Brillouin zone for all compounds. Also, the partial density of state indicates that the main contribution of the top valance band is the 5p state of halogen with little contribution of the 5s state. On the other hand, the main contribution of the conduction band arises from anti-bonding 5p states of the halogen atoms and 5S states of Sn atoms.

Solar cells

$((CH_3)_3S)_2SnX_6$ (X = Cl, Br, I, I_5Cl, I_4Cl_2, I_5Br, I_4Br_2) perovskites were employed as electrolyte-free based on Dye sensitized solar cells of the type **FTO/TiO_2-Dye//perovskite//Pt/FTO**, using the nanoparticulate TiO_2 films and different type of sensitization with either the metal-organic (Z907, N917) or the organic (MK2, N3 and D35) dyes.

From the JV plots the values of short-circuit current density (J_{sc}), open-circuit voltage (V_{oc}), fill factor (FF) and photovoltaic efficiency (PCE) were deduced and recorded in Table 1. The efficiency is defined as the ratio of the maximum electrical power produced by the cell (JV_{max}) over the incident light power (P), and it was achieved by equation (1):

$$PCE\ \% = \frac{(\mathrm{JV})\mathrm{max}}{\mathrm{P}} \times 100 \qquad (1)$$

For the calculation of the fill factor values we used the equation (2):

$$FF = \frac{(\mathrm{JV})\mathrm{max}}{\mathrm{J_{sc}V_{oc}}} \qquad (2)$$

Among different type of cells those which combine the Z907 sensitizer with the perovskite HTMs based on pure iodide and monosubstituted Bromide/chloride, achieved the highest performances, 5.07% and ~ 4%, correspondingly. The photovoltaic parameters are summarized in Table 1. The highest value of the photocurrent density, 20.05 mA cm^{-2}, was recorded for the pure iodide-based perovskite. This value was reduced to 14.03 and 12.06 mA cm^{-2} for monosubstituted bromide and chloride respectively. On the hand, Figure 3, shows that the quite high efficiency was observed for the N719 dye than organic MK2 and D35 dyes.

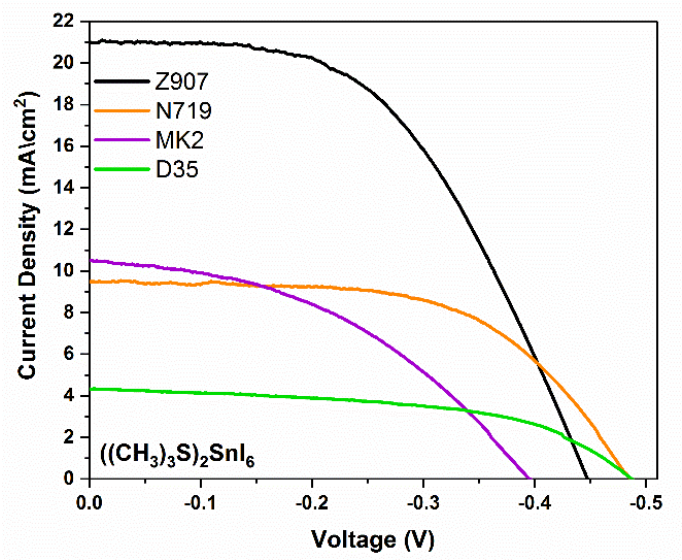

Figure 3. Photovoltaic performance of solar cells based on $((CH_3)_3S)_2SnI_6$ and various dyes.

Table 1. Photovoltaic performance of solar cells based on the title compounds based and various dyes.

Dye	Compound	J_{sc} (mA cm^{-2})	V_{oc} (V)	FF	PCE %
D35	$((CH_3)_3S)_2SnI_6$	4.34	0.49	0.53	1.12
MK2	$((CH_3)_3S)_2SnI_6$	10.5	0.4	0.42	1.77
N719	$((CH_3)_3S)_2SnI_6$	9.54	0.49	0.57	2.68
Z 907	$((CH_3)_3S)_2SnI_6$	20.05	0.48	0.53	5.07
	$((CH_3)_3S)_2SnI_5Br$	14.03	0.51	0.56	4.02

$((CH_3)_3S)_2SnI_4Br_2$	6.36	0.49	0.53	1.64
$((CH_3)_3S)_2SnI_5Cl$	12.06	0.55	0.6	4.00
$((CH_3)_3S)_2SnI_4Cl_2$	8.66	0.59	0.58	2.95

Conclusions

Lead-free, air-stable, low toxic $((CH_3)_3S)_2SnI_{6-x}Cl_x$ and $((CH_3)_3S)_2SnI_{6-x}Br_x$ (x= 0, 1, 2) defect perovskites have high potential for semiconducting applications. The photophysical characterization and DFT computational calculation confirm that the lattice vibrations modes and electronic bandgaps are between 1.38 and 1.5 eV and depend largely on the effect of mixing I and Cl/Br atoms. We utilize the title compounds as hole-transporting materials in electrolyte-free dye-sensitized solar cells, based on mesoporous titania electrodes with different type of sensitizer metal-organic (Z907, N719) and organic (MK2, D35) dyes. A power conversion efficiency (PCE) of 4% under the standard illumination conditions of 100 mW cm^{-2} were achieved for the $((CH_3)_3S)_2SnI_5Br$ and $((CH_3)_3S)_2SnI_5Cl$ layer sandwiched between the metal-organic Z907 and Pt interface. Electrochemical impedance results confirm low hole extraction resistance of mono-substituted halogen at the perovskite-Pt electrode. Overall, our results promote trimethyl sulfonium tin-based perovskites as chemically stable hole-transport material in lead free solar cells.

Acknowledgements

M. Elsenety is financially supported by Science Achievement Scholarship of High Education Ministry of Egypt in cooperation with the Hellenic Ministry of Foreign Affairs for his PhD Scholarship. This research has been co-financed by the European Regional Development Fund of the European Union and Greek national funds through the Operational Program Competitiveness, Entrepreneurship and Innovation, under the call RESEARCH – CREATE – INNOVATE (project code:T1EDK-03547)».

References:

[1] S. Il Seok, M. Grätzel, N.-G. Park. Small. 14 (2018) 1704177.

[2] https://www.nrel.gov/pv/assets/pdfs/best-reserch-cell-efficiencies.20190411.pdf

[3] P. Gao, M. Graetzel, M.K. Nazeeruddin. ENERGY Environ. Sci. 7 (2014) 2448–2463.

[4] M. Saliba, J.P. Correa-Baena, C.M. Wolff, M. Stolterfoht, N. Phung, S. Albrecht, D. Neher, A. Abate. Chem. Mater. 30 (2018) 4193–4201.

[5] J.-P. Correa-Baena, A. Abate, M. Saliba, W. Tress, T. Jesper Jacobsson, M. Grätzel. Energy Environ. Sci. 10 (2017) 710–727.

[6] M.A. Green, A. Ho-Baillie. ACS Energy Lett. 2 (2017) 822–830.

[7] S.D. Stranks, P.K. Nayak, W. Zhang, T. Stergiopoulos, H.J. Snaith. Angew. Chemie - Int. Ed. 54 (2015) 3240–3248.

[8] H.S. Jung, N.G. Park. Small. 11 (2015) 10–25.

[9] M. Grätzel. Nat. Mater. 13 (2014) 838–842.

[10] G. Niu, X. Guo, L. Wang. J. Mater. Chem. A. 3 (2015) 8970–8980.

[11] B. Lee, C.C. Stoumpos, N. Zhou, F. Hao, C. Malliakas, C.Y. Yeh, T.J. Marks, M.G. Kanatzidis. J. Am. Chem. Soc. 136 (2014) 15379–15385.

[12] A. Kaltzoglou, M. Antoniadou, A.G. Kontos, C.C. Stoumpos, D. Perganti, E. Siranidi, V. Raptis, K.

Trohidou, V. Psycharis, M.G. Kanatzidis, P. Falaras. J. Phys. Chem. C. 120 (2016) 11777–11785.

[13] M.M. Elsenety, A. Kaltzoglou, M. Antoniadou, I. Koutselas, A.G. Kontos, P. Falaras. Polyhedron. 150 (2018) 83–91.

[14] A. Kaltzoglou, M.M. Elsenety, I. Koutselas, A.G. Kontos, C.P. Raptopoulou, K. Papadopoulos, D. Perganti, T. Stergiopoulos, V. Psycharis, P. Falaras. Polyhedron. 140 (2017) 67–73.

[15] M.D. Segall, P.J.D. Lindan, M.J. Probert, C.J. Pickard, P.J. Hasnip, S.J. Clark, M.C. Payne. J. Phys. Condens. Matter. 14 (2002) 2717–2744.

[16] B. Saparov, D.B. Mitzi. Chem. Rev. 116 (2016) 4558–4596.